Volume 9, Issue 2, 092510 (128-137)

Trends in Phytochemical Research (TPR)

https://doi.org/10.57647/tpr.2025.0902.10

Characterization, quantification and antioxidant potential of phenolic compounds in *Brachychiton rupestris* (T.Mitch. ex Lindl.) K. Schum. leaves

Heba Raafat Mohamed[1,*], Eman Ahmed El-Wakil[1], Maher Mahmoud El-Hashash[2], El-Sayed Saleh Abdel-Hameed[1]

[1]*Department of Medicinal Chemistry, Theodor Bilharz Research Institute, Korniash El-Nile, Giza, Egypt.*
[2]*Department of Chemistry, Faculty of Science, Ain-Shams University, El-Khalifa El-Mamoun, Cairo, Egypt.*

[*]**Corresponding author:** hebaraafat_p@sci.asu.edu.eg

Original Research

Received:
10 October 2024
Revised:
18 June 2025
Accepted:
23 June 2025
Published online:
24 June 2025

© 2025 The Author(s). Published by the OICC Press under the terms of the Creative Commons Attribution License, which permits use, distribution and reproduction in any medium, provided the original work is properly cited.

Abstract:

The studies conducted to investigate the pharmacological potential or the chemical composition of *Brachychiton rupestris* leaves were very limited. The present study aims to isolate, identify and quantify the major phenolics in *B. rupestris* leaves and to evaluate their antioxidant potential. Methanol (85.0%) extract of *B. rupestris* leaves was prepared and successively partitioned with petroleum ether, dichloromethane, ethyl acetate and *n*-butanol, respectively. The bioactive compounds in the ethyl acetate and *n*-butanol fractions were separated chromatographically, and their structures were characterized. Their concentrations were determined using HPLC-DAD, and their antioxidant potential was evaluated against DPPH$^{\cdot}$. Caffeic acid, *p*-coumaric acid, nicotiflorin, methyl gallate, isoquercetin, rutin, quercetin and kaempferol were the major phytochemicals. Methyl gallate exhibited the most potent antioxidant activity with an IC_{50} of 18.19 ± 0.161 µg/mL. *B. rupestris* could be considered a promising source of antioxidants which suggests its application in nutraceuticals and therapeutic formulations.

Keywords: Antioxidant; *Brachychiton rupestris* (T.Mitch. ex Lindl.) K. Schum.; Caffeic acid; HPLC-DAD; Malvaceae; Methyl gallate; Nicotiflorin

1. Introduction

Reactive oxygen and nitrogen species (RONS) are highly reactive oxidants normally produced within the human body as a result of normal metabolic processes such as aerobic respiration or as a response to external stimuli such as exposure to ionizing radiations or other environmental pollutants. Numerous researches have linked the overproduction of RONS that exceeds the antioxidative capability of the body to the pathogenesis of many serious diseases including diabetes, cancer, asthma, rheumatoid arthritis, renal, cardiovascular and eye disorders and premature senescence (Phaniendra et al., 2015; Atta et al., 2017).

The rising incidence of chronic, infectious, and drug-resistant diseases has intensified the demand for effective, powerful, safe, and affordable therapeutic alternatives. Medicinal plants offer sustainable healthcare solutions to emerging health threats and serve as a viable alternative to synthetic drugs, owing to their abundance of bioactive compounds that exhibit diverse pharmacological activities, including antioxidant, anti-inflammatory, antifungal, anti-cancer, antiviral, antibacterial, anti-diabetic, hypotensive, and immunomodulatory properties. Given their historical use in traditional medicine and growing scientific validation, medicinal plants continue to be a significant resource for drug development and integrative medicine, bridging traditional knowledge with scientific evidence (Mohammadhosseini et al., 2021; Thagriki et al., 2022; Mohammadhosseini et al., 2023). Medicinal plants are rich in a variety of secondary metabolites that possess remarkable therapeutic and healing properties. Among these bioactive phytocompounds are phenolic acids, flavonoids, and carotenoids, which are known to be potent antioxidant agents. Therefore, medicinal plants could serve as an excellent alternative to counteract the deleterious effects of RONS on health (Yasir

et al., 2016).

Brachychiton rupestris (T.Mitch. ex Lindl.) K. Schum., also known as "Queensland bottle tree", is a flowering plant native to Queensland in Australia with a bottle shaped trunk. It belongs to family Malvaceae within a small genus "*Brachychiton*" which comprises about 30 species. Generally, few studies have been conducted to investigate the pharmacological potential and/or to identify the phytochemical composition of *B. rupestris*. According to these studies, *B. rupestris* was found to possess significant antioxidant, antimicrobial and cytotoxic activities in addition to strong antischistosomal potential on *Schistosoma mansoni* and potent hypoglycemic and hepatoprotective action on experimental animals (El-Sherei et al., 2016; Zeid et al., 2017; Thabet et al., 2017; Mohamed et al., 2021). The secondary metabolites isolated and identified from *B. rupestris* could be categorized into four main groups which are phenolics, flavonoids, sterols and volatile compounds (Farag et al., 2014; Thabet et al., 2018b; Thabet et al., 2018a; Ragheb et al., 2019; Rjeibi et al., 2020). Recent investigations on species of family Malvaceae indicated their anti-inflammatory and anthelminthic potential (Anish et al., 2023; Gurivelli et al., 2023).

According to our knowledge, there are no previous reports on the antioxidant potential of the phenolics isolated from *B. rupestris* leaves cultivated in Egypt. Therefore, the current study was performed to explore the antioxidant activity of the phenolics isolated from the ethyl acetate and the *n*-butanol fractions derived from the methanol extract of *B. rupestris* leaves via *in-vitro* antioxidant assay. The predominant phenolic compounds were isolated, purified and quantified in the two bioactive fractions through combination of various chromatographic techniques and their chemical structures were identified via different spectral analyses.

2. Experimental

2.1 Chemicals and reagents

DPPH (1,1'-diphenyl-2-picrylhydrazyl radical) was purchased from Sigma-Aldrich (Steinheim, Germany); Organic solvents: Methanol, petroleum ether (60-80 °C), ethyl acetate, *n*-butanol, methylene chloride, sulfuric acid, acetic acid all were of analytical chemical grade obtained from El-Nasr Pharmaceutical Chemicals Co., Egypt; Adsorbents: Polyamide 6S (high purity grade) for column chromatography was purchased from Riedel-De Haën AG, Seelze-Hannover, Germany, Lipophilic sephadex LH-20, silica gel 90 C_{18}-reversed phase for column chromatography and ready-made silica gel TLC cards (with fluorescent indicator at 254 nm, layer thickness 0.2 mm, 20 × 20 cm aluminum cards were purchased from Sigma-Aldrich, Germany and Whatmann filter papers No. 1 and 3 mm for paper chromatography were purchased from England.

2.2 Plant material

Leaves of *B. rupestris* were collected, in September 2017, from Orman Garden, Giza, Egypt (30° 01′ 45.0″ N, 31° 12′ 47.0″ E). Both Mrs. Treaze Labib (a consultant of plant taxonomy at Agriculture Ministry and the ex-director of Orman Garden) and Mrs. Rehab Mohamed Eid (a botanist at Orman Garden Herbarium) performed the identification process of a plant specimen and a voucher sample was deposited at Orman Garden Herbarium (No. 278 BC). The collected plant leaves were shade dried at room temperature and were then blended to coarse powder using electric blender.

2.3 Extraction and fractionation processes

The plant leaves as a fine powder (2.0 kg) were successively extracted with 85% aqueous methanol at room temperature. The resulting extract was then filtered and evaporated under reduced pressure using a rotary evaporator (BUCHI, Germany) until complete dryness was achieved, yielding a crude methanol extract of 335 g (16.79%). The crude extract was subsequently fractionated successively using petroleum ether, methylene chloride, ethyl acetate, and *n*-butanol. The fractions were then evaporated under reduced pressure until complete dryness was achieved, yielding approximately 10 g of petroleum ether, 27 g of methylene chloride, 9.0 g of ethyl acetate, 45 g of *n*-butanol, and 111 g of aqueous fractions. The ethyl acetate as well as the *n*-butanol derived fractions were chosen to further chromatographic analyses due to their strong antioxidant and cytotoxic activities which may be attributed to their richness with phenolics (Mohamed et al., 2021).

2.4 Chromatographic isolation of compounds from bioactive fractions

The ethyl acetate fraction (5.0 g) and the *n*-butanol fraction (35 g) were loaded separately into two chromatography columns (3 × 58 and 5 × 106 cm, respectively) filled with polyamide. Elution was started with distilled water followed by mixtures of water and methanol with decreasing polarity and ended with 100% methanol. Similar fractions on PC and TLC were collected. Promising groups were re-chromatographed on sephadex LH-20 and RP-C_{18} silica gel and their products were monitored on PC and TLC. Five compounds were separated from the ethyl acetate fraction and three compounds were separated from the *n*-butanol fraction; Kaempferol (**1**) and quercetin (**6**) were eluted with MeOH (5.0%). Rutin (**7**) was eluted with 5-10% methanol. Caffeic acid (**2**) and *p*-coumaric acid (**3**) were eluted with 10-20% methanol. Furthermore, methyl gallate (**4**) and nicotiflorin (**8**) were eluted with 20-40% methanol while isoquercetin (**5**) was eluted with 40-60% MeOH. All separated compounds were purified through applying over sephadex LH-20 sub columns except for compounds **4** and **8** which were purified with RP-C_{18} silica gel sub column, after first purification with sephadex. The physical properties of each compound including color and retention factor (R_f) in three different eluting systems were detected. The used eluting systems were; 15% AcOH (S_1, PC), BAW (S_2, PC) and EtOAc:MeOH:H_2O (8:1:1) (S_3, TLC). The structures of the purified compounds were identified by various spectroscopic tools including UV, NMR and TLC-MS analyses. HPLC-DAD was used to confirm the purity of the isolated compounds and to estimate their concentration in both the crude extract and the fraction from which they were separated, based on their retention time (R_t) and the area under the peak. The flowchart of the extraction, fractionation,

chromatographic isolation and purification of phenolic compounds from *B. rupestris* leaves is represented in Fig. 1.

2.5 Equipment and conditions of spectroscopic analyses

2.5.1 NMR spectrometer

The proton and carbon patterns of the isolated pure compounds were identified throug ^{1}H-NMR spectrometer (Bruker Avance (III) NMR spectrometer, USA) 400 MHz for ^{1}H-NMR and 100 MHz for ^{13}C-NMR. All analyzed compounds were dissolved in DMSO-d_6. The chemical shifts of the compounds' peaks were expressed in δ_{ppm}, using TMS as the internal standard, and their coupling constants (J) were expressed in Hz. The spectra were processed via MestReNova 6.0.2 software.

2.5.2 Thin layer chromatography hyphenated with mass spectrometer (TLC-MS)

The molecular ion peaks as well as the fragmentation patterns of the isolated pure compounds were obtained through TLC-MS apparatus as follows; a readymade silica gel TLC card was prepared by loading the purified compounds, previously dissolved in highly purified methanol, using clean capillary tubes which was then subjected to the TLC-MS apparatus (Advion compact mass spectrometer (CMS) NY, USA), at Nawah Scientific, that eluted each spot, separately with methanol by the assistance of the pump that was attached to the device at a flow rate of 10 µL/min to 1 mL/min into the ESI mass spectrometer. The mass spectra were detected in the ESI (negative mode) within the range of 100 to 1200 *m/z*. The peaks and the spectra were processed using the CheMass and Advion Data Express software.

2.5.3 High performance liquid chromatography hyphenated with photodiode array detector (HPLC-DAD)

The methanol extract, the ethyl acetate, the *n*-butanol derived fractions as well as the compounds isolated and purified from *B. rupestris* fractions were dissolved in HPLC grade MeOH at known concentrations, filtered using a filter membrane (pore size 0.45 µm, Phenex, USA) and centrifuged for 5 min at 8,050 × g then injected to the HPLC apparatus; HPLC-DAD (LC-8A liquid chromatography system hyphenated with SPD-M20A photodiode array detector Shimadzu, Kyoto, Japan) with LC solution software. The chromatographic separation was performed through RESTEK RP-C_{18} analytical column (4.6 × 150 mm, particle size 5 µm) and the elution occurred at a flow rate of 1 mL/min. The solvent system consisted of gradient mixtures of methanol (B) and acidified water with 0.1% formic acid (A) starting with 5% B at 0-5 min, 5-34% B at 5-32 min, 34-40% B at 32-50 min, 40-46% B at 50-55 min, 46-80% B at 55-65 min and 80-100% B at 65-68 min. The eluate was monitored at 210 and 280 nm for the detection of the major chemical constituents in the plant extract and both fractions. The injection volume was 40 µL and the total run time was 68 min. The R_t and the area under the peaks corresponding to the purified compounds were recorded, allowing for the calculation of their concentrations in both the crude extract and the fractions from which they were separated. The column was reconditioned for 10 min before each analysis. All chromatographic operations were conducted at ambient temperature.

2.6 Estimation of *in vitro* antioxidant potential

2.6.1 DPPH radical scavenging activity

The antioxidant potential of the pure isolated compounds was evaluated based on their ability to neutralize DPPH• (1,1'-diphenyl-2-picryl hydrazyl radical), a stable dark purple radical that converts to yellow upon reduction. Different concentrations of the isolated compounds in methanol were mixed with freshly prepared DPPH solution in methanol (0.09 mM) in a ratio of 1:1 according to the method described by Mohamed et al. (2023). The reaction mixtures were allowed to stand for 30 minutes in dark at room temperature then the decrease in the optical density was measured

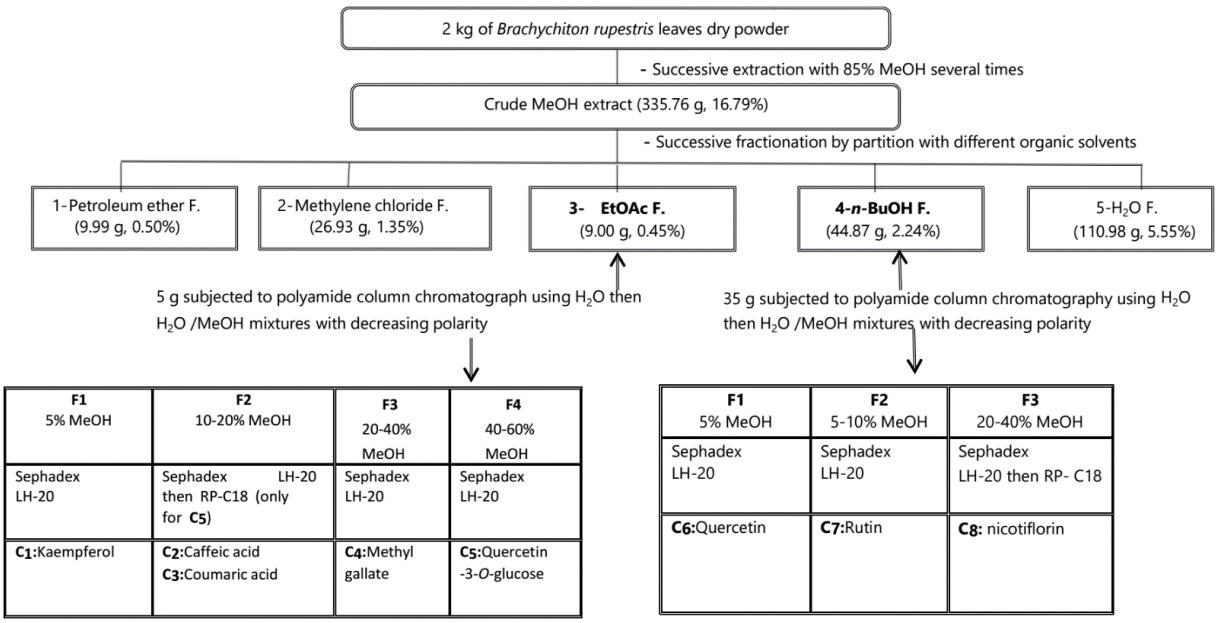

Figure 1. Flowchart of extraction, fractionation and isolation of active constituents from *B. rupestris* leaves.

at 517 nm against blank. Ascorbic acid (AA) was used as a positive control. The scavenging ability of the isolated compounds toward DPPH• was calculated according to Eqn. (1):

$$\text{DPPH}^{\bullet}\text{ scavenging activity}\% = \left(\frac{A_{control} - A_{sample}}{A_{control}}\right) \times 100 \quad (1)$$

Where $A_{control}$ is the absorbance of the control solution containing methanol instead of test sample while A_{sample} is the absorbance of the isolated compound. The determinations were carried out in triplicates and the results were expressed as SC_{50} which is the concentration of the plant sample required to reduce half of DPPH•.

2.7 Statistical analysis

The statistical analyses were carried out using IBM SPSS Statistics (25) software. The results were expressed as means ± standard deviation (SD) and all experimental analyses were performed in triplicate.

2.8 Spectroscopic data of the separated pure compounds

Caffeic acid (2): White powder (18 mg). R_f values: 0.61 (15% AcOH (S_1, PC)), 0.87 (BAW (S_2, PC)) and 0.80 (EtOAc: MeOH: H_2O (8:1:1) (S_3, TLC)). Color UV blue. UV (MeOH): λ_{max} 218, 240, 325 nm. $C_9H_7O_4$, negative ESI-MS *m/z* 178.9 [M-H]$^-$; MS^2 *m/z* 135.11 [M-H-CO_2]. ^{1}H-NMR (400 MHz, d_6-DMSO): δ_H 10.36 (2H, br s, OH-3, 4), 7.41 (1H, br d, *J* = 15.9 Hz, H-7), 7.03 (1H, d, *J* = 2.1 Hz, H-2), 6.96 (1H, dd, *J* = 8.4, 2.1 Hz, H-6), 6.79 (1H, d, *J* = 8.4 Hz, H-5), 6.18 (1H, br d, *J* = 15.9 Hz, H-8). ^{13}C-NMR (100 MHz, d_6-DMSO): δ_c 168.51 (C-9), 148.60 (C-4), 146.05 (C-7), 144.51 (C-3), 126.19 (C-1), 121.58 (C-6), 116.22 (C-5), 115.97 (C-2), 115.09 (C-8).

***p*-Coumaric acid (3):** White powder (24 mg). R_f values: 0.81 (15% AcOH (S_1, *P*C)), 0.93 (BAW (S_2, PC)) and 0.87 (EtOAc: MeOH: H_2O (8:1:1) (S_3, TLC)). Color UV light blue. UV (MeOH): λ_{max} 210, 224, 310 nm. $C_9H_7O_3$, negative ESI-MS *m/z* 162.90 [M-H]$^-$; MS^2 *m/z* 119.13 [M-H-CO_2]. ^{1}H-NMR (400 MHz, d_6-DMSO): δ_H 10.30 (1H, br s, OH-4), 7.51 (2H, d, *J* = 7.9 Hz, H-2, H-6), 7.41 (1H, br d, *J* = 15.9 Hz, H-7), 6.79 (2H, d, *J* = 8.4 Hz, H-3, 5), 6.29 (1H, br d, *J* = 15.9 Hz, H-8); ^{13}C-NMR (100 MHz, d_6-DMSO): δ_c 168.51 (C-9), 160.04 (C-4), 146.05 (C-7), 116.22 (C-3), 125.76 (C-1), 130.52 (C-6), 116.22 (C-5), 130.52 (C-2), 115.74 (C-8).

Methyl gallate (4): Brown powder (18 mg). R_f values: 0.63 (15% AcOH (S_1, PC)), 0.92 (BAW (S_2, PC)) and 0.82 (EtOAc: MeOH: H_2O (8:1:1) (S_3, TLC)). Color UV blue. UV (MeOH): λ_{max} 207, 272 nm. $C_8H_8O_5$, negative ESI-MS *m/z* 182.90 [M-H]$^-$; MS^2 *m/z* 124.08 [M-H-CO_2-CH_3]$^-$. ^{1}H-NMR (400 MHz, d_6-DMSO): δ_H 6.92 (2H, s, H-2, 6), 3.74 (3H, s, OCH_3). ^{13}C-NMR (100 MHz, d_6-DMSO): δ_c 166.54 (C-7), 145.75 (C-3, 5), 138.78 (C-4), 119.34 (C-1), 108.89 (C-2, 6), 51.75 (C-8).

Isoquercetin (Quercetin-3-*O*-β-D-glucopyranoside) (5): Yellow amorphous powder (42 mg). R_f values: 0.54 (15% AcOH (S_1, PC)), 0.76 (BAW (S_2, PC)) and 0.55 (EtOAc: MeOH: H_2O (8:1:1) (S_3, TLC)). Color UV dark purple. UV (MeOH): λ_{max} (nm) 256, 295^{Sh}, 354; NaOMe: 271, 325^{Sh}, 403; $AlCl_3$: 273, 303^{Sh}, 332, 433; $AlCl_3$/HCl: 271, 301^{Sh}, 355, 401; NaOAc: 270, 320^{Sh}, 375; NaOAc/H_3BO_3: 265, 298^{Sh}, 375. $C_{21}H_{19}O_{12}$; negative ESI-MS *m/z* 463 [M-H]$^-$; MS^2 *m/z* 301 [M-H]$^-$ glucosyl moiety (162 amu)]$^-$ and *m/z* 255 [M-H-glucosyl- CO_2-H]$^-$. ^{1}H-NMR (400 MHz, d_6-DMSO): δ_H 12.63 (1H, s, OH-5), 7.59 (1H, dd, *J* = 8.2, 2.0 Hz, H-6′), 7.57 (1H, d, *J* = 2.0 Hz, H-2′), 6.85 (1H, d, *J* = 8.2 Hz, H-5′), 6.40 (1H, d, *J* = 1.6 Hz, H-8), 6.18 (1H, d, *J* = 1.6 Hz, H-6), 5.45 (1H, d, *J* = 7.2 Hz, H-1″), 3.58 (2H, d, *J* = 11.3 Hz, H-6″), 3.35 (1H, d, *J* = 4.3 Hz, H-2″), 3.32 (1H, d, *J* = 4.7 Hz, H-3″), 3.24 (1H, d, *J* = 5.2 Hz, H-4″), 3.09 (1H, s, H-5″). ^{13}C-NMR (100 MHz, d_6-DMSO): δ_c 177.81 (C-4), 165.07 (C-7), 161.61 (C-5), 156.83 (C-2), 156.66 (C-9), 148.97 (C-4′), 145.27 (C-3′), 133.71 (C-3), 122.06 (C-6′), 121.55 (C-1′), 116.60 (C-5′), 115.71 (C-2′), 104.25 (C-10), 101.35 (C-1″), 99.30 (C-6), 94.12 (C-8), 77.85 (C-3″), 76.87 (C-5″), 74.52 (C-2″), 70.28 (C-4″), 61.32 (C-6″).

Rutin (quercetin-3-*O*-rutinoside) (7): Yellow powder (42 mg). R_f values: 0.68 (15% AcOH (S_1, PC)), 0.73 (BAW (S_2, PC)) and 0.29 (EtOAc: MeOH: H_2O (8:1:1) (S_3, TLC)). Color UV dark purple. UV (MeOH): λ_{max} (nm) 256, 300^{Sh}, 354; NaOMe: 272, 325^{Sh}, 408; $AlCl_3$: 274, 305^{Sh}, 432; $AlCl_3$/HCl: 270, 301^{Sh}, 360, 403; NaOAc: 273, 325^{Sh}, 389; NaOAc/ H_3BO_3: 257, 300^{Sh}, 380. $C_{27}H_{29}O_{16}$, negative ESI-MS *m/z* 609 [M-H]$^-$; MS^2 *m/z* 463 [M-H]$^-$ rhamnosyl moiety (146 amu)]$^-$ and 301[M-H- rhamnosyl and glucosyl moieties (146-162)]$^-$. ^{1}H-NMR (400 MHz, d_6-DMSO): δ_H 12.60 (1H, s, OH-5), 10.90 (1H, s, OH-7), 10.14 (1H, s, OH-4′), 9.23 (1H, s, OH-3′), 7.56 (1H, dd, *J* = 8.5, 2.0 Hz, H-6′), 7.54 (1H, d, *J* = 2.0 Hz, H-2′), 6.85 (1H, d, *J* = 8.5 Hz, H-5′), 6.39 (1H, d, *J* = 2.1 Hz, H-8), 6.20 (1H, d, *J* = 2.1 Hz, H-6), 5.35 (1H, d, *J* = 7.2 Hz, H-1″), 5.08 (1H, d, H-1‴), 4.39-3.05 (10H, m), 0.99 (3H, d, *J* = 6.2 Hz, 6‴-CH_3); ^{13}C-NMR (100 MHz, d_6-DMSO): δ_c 177.83 (C-4), 164.55 (C-7), 161.68 (C-5), 156.88 (C-2), 156.88 (C-9), 148.87 (C-4′), 145.21 (C-3′), 133.77 (C-3), 122.15 (C-6′), 121.64 (C-1′), 116.73 (C-5′), 115.69 (C-2′), 104.43 (C-10), 101.65 (C-1‴), 101.21 (C-1″), 99.14 (C-6), 93.66 (C-8), 76.92 (C-3″), 76.37 (C-5″), 74.53 (C-2″), 72.31 (C-4‴), 71.02 (C-4″), 70.83 (C-2‴), 70.46 (C-3‴), 68.70 (C-5‴), 67.44 (C-6″), 18.19 (C-6‴).

Nicotiflorin (kaempferol-3-*O*-rutinoside) (8): Black powder (50 mg). R_f values: 0.69 (15% AcOH (S_1, PC)), 0.75 (BAW (S_2, PC)) and 0.40 (EtOAc: MeOH: H_2O (8:1:1) (S_3, TLC)). Color UV dark purple. UV (MeOH): λ_{max} (nm) 265, 295^{Sh}, 348; NaOMe: 275, 325^{Sh}, 404; $AlCl_3$: 265, 305^{Sh}, 349, 400; $AlCl_3$/HCl: 265, 305^{Sh}, 350, 398; NaOAc: 275, 304^{Sh}, 386; NaOAc/ H_3BO_3: 265, 295^{Sh}, 350. $C_{27}H_{29}O_{15}$, negative ESI-MS *m/z* 593 [M-H]$^-$; MS^2 *m/z* 447 [M-H-rhamnosyl moiety (146 amu)]$^-$ and 285[M-H-rhamnosyl and glucosyl moieties (146-162)]$^-$. ^{1}H-NMR (400 MHz, d_6-DMSO): δ_H 12.56 (1H, s, OH-5), 10.89 (1H, s, OH-7), 10.15 (1H, s, OH-4′), 7.98 (2H, d, *J* = 8.2 Hz, H-2′, 6′), 6.89 (2H, d, *J* = 7.7 Hz, H-3′, 5′), 6.43 (1H, d, H-8), 6.21 (1H, d, H-6), 5.31 (1H, d, *J* = 7.1 Hz, H-1″), 5.09 (1H, d, H-1‴), 4.55-3.08 (10 H, m), 1.05 (3H, d, *J* = 6.3 Hz, CH_3-6‴). ^{13}C-NMR (100 MHz, d_6-DMSO): δ_c 177.83 (C-4), 164.53 (C-7), 161.57 (C-5), 160.27 (C-4′), 157.42 (C-2), 156.96 (C-

9), 133.62 (C-3), 131.35 (C-2′, 6′), 121.33 (C-1′), 115.58 (C-3′, 5′), 104.44 (C-10), 101.73 (C-1‴), 101.16 (C-1″), 99.21 (C-6), 94.26 (C-8), 76.74 (C-3″), 76.09 (C-5″), 74.57 (C-2″), 72.24 (C-4‴), 71.01 (C-4″), 70.75 (C-2‴), 70.35 (C-3‴), 68.66 (C-5‴), 67.35 (C-6″), 18.05 (C-6‴).

Two aglycones were separated, purified, and identified based on the UV-Vis spectral analysis using different diagnostic shift reagents and co-PC, as well as co-TLC using authentic samples of kaempferol (**1**, 11 mg) and quercetin (**6**, 30 mg).

3. Results and discussion

Eight compounds were isolated and purified from *B. rupestris* leaves via application of various chromatographic techniques such as conventional column chromatography (CC), paper chromatography (PC) and thin layer chromatography (TLC). Five compounds were separated from the ethyl acetate fraction, in addition to three other compounds obtained from the *n*-butanol fraction, which were derived from the crude methanol extract of the plant leaves. These compounds were structurally identified through different spectroscopic analyses including TLC-MS, UV-vis, ^{1}H-NMR

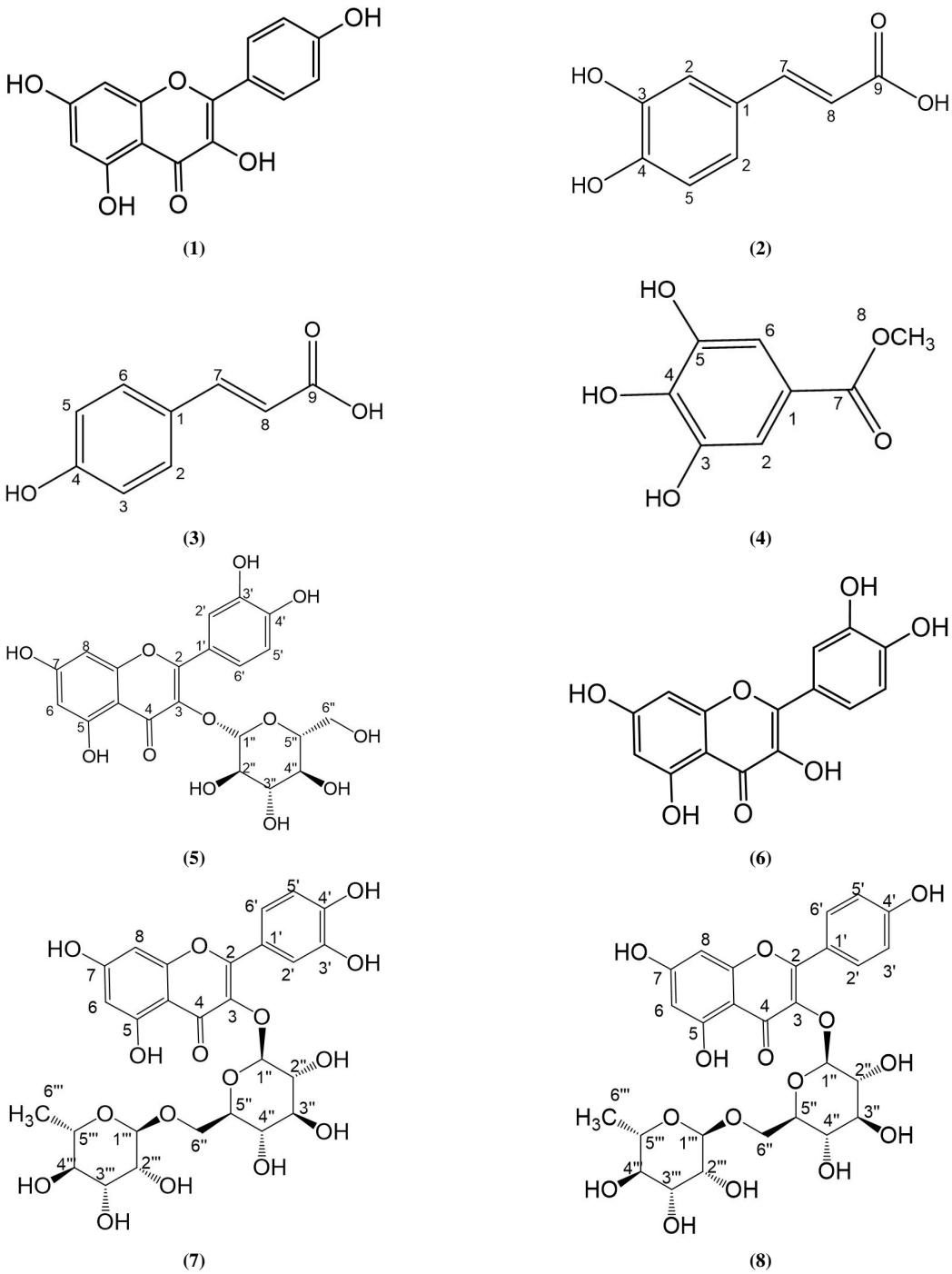

Figure 2. Isolated compounds from *B. rupestris* leaves.

and ^{13}C-NMR analyses.

Compound 1 was isolated as a yellow amorphous powder, which appeared as a yellow spot on PC that did not change upon spraying with $AlCl_3$. Depending on the co-PC, co-TLC, the above mentioned data and the comparison with published literature, compound **1** was elucidated as kaempferol (Iwashina et al., 2013). Kaempferol has previously been isolated before from *B. acerifolius* (Farag et al., 2014; Zeid et al., 2017), *B. rupestris* (El-Sherei et al., 2016) and *B. populneus* (Ragheb et al., 2019).

Compound 2 was isolated as a white powder, which appeared as a blue spot on PC and was not affected by spraying. The negative mode of ESI-MS spectrum showed a molecular ion peak [M-H]$^-$ at *m/z* 178.9 so that the molecular formula is suggested to be $C_9H_7O_4$. Also, the molecule ion peak is fragmented in the negative mode of LC-ESI-MS producing a peak at *m/z* 135.11 [M-H-CO_2] due to loss of carbon dioxide molecule. The ^{1}H-NMR of the compound dissolved in DMSO-d_6 showed two doublet signals at δ_H 7.41 and 6.18 ppm, with a coupling constant (J) of 15.9 Hz which is characteristic of the *trans* olefinic protons found in hydroxycinnamic acids. One more doublet signal was observed at δ_H 6.79 ppm with coupling constants (J) of 8.4 Hz corresponding to H-5 whille a doublet of doublet signal was detected at δ_H 6.96 ppm with coupling constants (J) of 8.4 and 2.1 Hz corresponding to H-6. Additionally, a doublet signal at δ_H 7.03 ppm indicated the presence of a 1,3,4-trisubstituted phenyl unit. The broad singlet at δ_H 10.36 ppm with 2H suggested the presence of two hydroxyl groups (3-OH, 4-OH). The ^{13}C-NMR of the compound in DMSO-d_6 exhibited nine signals with characteristic signal at δ_C 168.51ppm corresponding to carbonyl carbon of carboxylic group. The rest carbon signals cope with those of 3,4-dihydroxycinnamic acid (caffeic acid). Compound **2** was confirmed to be caffeic acid (Jeong et al., 2011; Wang et al., 2012), which had previously been identified in *B. acerifolius* (Farag et al., 2014) and *B. populneus* (Rjeibi et al., 2020). As far as we know, this is the first time it has been isolated from *B. rupestris*.

Compound 3 was separated as a white powder that appeared as light blue spot on PC and retained its blue color after spraying. The precursor ion [M-H]$^-$ of the compound in methanol appeared at *m/z* 162.90 in the ESI-MS spectrum (negative mode), indicating a molecular formula of $C_9H_7O_3$. The molecule ion is fragmented, producing a daughter ion at *m/z* 119.13 [M-H-CO_2]$^-$ in the negative mode of LC-MS. The ^{1}H-NMR of the compound in DMSO-d_6 exhibited two doublet signals with a coupling constant of 15.9 Hz at δ_H 7.41 and 6.29 ppm, which are indicative of the two *trans* protons of the double bond present in hydroxycinnamic acids. Moreover, two additional doublets with coupling constant of 7.9 and 8.4 Hz at δ_H 7.51 and 6.79 ppm were recorded in the spectrum that indicated the *p*-substituted phenyl unit. The ^{13}C-NMR spectrum (DMSO-d_6) showed seven carbon atoms, four signals for the 1,4-disubstituted benzene ring, two signals corresponding to the two sp^2 carbons of olefinic bond and one signal for carbonyl carbon which resonances at δ_C 168.51 ppm. Compound **3** was elucidated as *p*-coumaric acid (Olennikov et al., 2018) that was previously reported in *B. rupestris* (Thabet et al., 2018a).

Compound 4 was isolated as a brown powder that appeared on PC as a blue spot that did not change after $AlCl_3$ spraying. It had a molecular formula of $C_8H_8O_5$ as its ESI-MS spectrum exhibited a molecule ion peak [M-H]$^-$ at *m/z* 182.90. Also, the molecule ion peak (*m/z* 183.14) is fragmented in the negative mode of LC-ESI-MS producing a peak at *m/z* 124.08 [M-H-CO_2-CH_3] due to loss of carbon dioxide molecule and methyl group which suggest the presence of acetoxy group. The ^{1}H-NMR spectrum of the compound dissolved in DMSO-d_6 showed one singlet signal at the aromatic region δ_H 6.92 ppm corresponding to two symmetrical aromatic protons at position 2 and 6. Moreover, one additional singlet signal corresponding to 3H at δ_H 3.74 ppm revealed the presence of one methoxy group. Six signals appeared in the ^{13}C-NMR spectrum of the compound in DMSO-d_6 indicating the presence of four aromatic carbons at δ_C (ppm); 108.89(C-2, C-6), 119.34 (C-1), 138.78 (C-4), 145.75 (C-3, C-5) in addition to one carbonyl carbon (C-7) at δ_C 166.54 ppm and one methoxy group (C-8) at δ_C 51.75 ppm. Compound **4** was recognized as the methyl ester of gallic acid (Lubis et al., 2018). This is the first time methyl gallate has been isolated from *B. rupestris*.

Compound 5 was obtained as yellow amorphous powder that appeared as a dark purple spot on PC that turned yellow on complexing with $AlCl_3$ spraying agent. The deprotonated molecular ion peak [M-H]$^-$ appeared in the negative mode of ESI-MS at *m/z* 463 which is consistent with the molecular formula of $C_{21}H_{19}O_{12}$. It was further fragmented into two molecule ions of *m/z* 301 [M-H-162]$^-$ and 255 due to loss of glucosyl moiety (162 amu) and subsequent loss of a proton and a carbon dioxide molecule [M-H-glucosyl- CO_2-H]$^-$. The ^{1}H-NMR of the compound (DMSO-d_6) showed a downfield singlet at δ_H 12.63 ppm attributed to 5-OH. Two *meta*-coupled protons appeared as doublets at δ_H 6.18 and 6.40 ppm with J 1.6 Hz corresponding to 6-H and 8-H. Also, the three aromatic protons of ring B appeared forming an ABX system at δ_H (ppm) 6.85 (d, J = 8.2 Hz, 1H, 5′-H), 7.57 (d, J = 2.0 Hz, 1H, 2′-H) and 7.59 (dd, 1H, J = 8.2, 2.0 Hz, 6′-H). Moreover, a set of signals that appeared in the region δ_H 3.58-3.09 ppm reflected the glycoside unit. The anomeric proton at δ_H 5.45 ppm which appeared as doublet with J = 7.2 Hz together with the ^{13}C-NMR chemical shifts of sugar unit carbons revealed that the sugar unit is O-β-D-glucopyranoside. The rest signals of ^{13}C-NMR were in complete agreement with those of quercetin aglycone. The downfield shift of both C-4 and C-2 and the upfield shift of C-3 in comparison with the aglycone indicated that the glucosyl moiety is attached to C-3. Compound **5** was identified as isoquercetin (Liu et al., 2010; Manivannan et al., 2015; Aisyah et al., 2017) which was previously separated from *B. rupestris* (Thabet et al., 2018a).

Compound 6 was identified as quercetin based on co-PC and co-TLC with quercetin authentic sample. Quercetin was previously reported in *B. acerifolius* (Farag et al., 2014; Zeid et al., 2017), *B. rupestris* (El-Sherei et al., 2016) and *B. populneus* (Ragheb et al., 2019).

Compound 7 was isolated as a yellow powder, which ap-

peared on PC as a dark purple spot that turned yellow upon spraying with $AlCl_3$. The ESI-MS (negative mode) exhibited the molecular ion at *m/z* 609 with a molecular formula of $C_{27}H_{29}O_{16}$. The molecule ion [M-H]$^-$ was broken apart giving two molecule ions at *m/z* 463 and 301 revealing the loss of rhamnosyl (146 amu) and glucosyl (162 amu) units, respectively. The ^{1}H-NMR (DMSO-d_6) displayed the characteristic signals of quercetin at δ_H (ppm); 12.60 (s, 1H, 5-OH), 10.90 (s, 1H, 7-OH), 10.14 (s, 1H, 4′-OH), 9.23 (s, 1H, 3′-OH), 7.56 (dd, 1H, 6′-H), 7.54 (d, J = 2.0 Hz, 1H, 2′-H), 6.85 (d, J = 8.5 Hz, 1H, 5′-H), 6.39 (d, 1H, J = 2.1 Hz, 8-H), 6.20 (d, 1H, J = 2.1 Hz, 6-H). The two anomeric protons of glucosyl and rhamnosyl moieties appeared at δ_H (ppm) 5.35 (d, J = 7.2 Hz, 1H) and 5.08 (d, 1H), respectively. The protons of the methyl group of rhamnose sugar appeared as doublet signal at δ_H 0.99 ppm. The ^{13}C-NMR spectrum was in full agreement with the reported spectra of rutin. The attachment of α-L-rhamnose to β-D-glucose was identified by the downfield shift of C-6″ of glucose. Compound **7** was identified as rutin (Oliveira et al., 2013; Ganbaatar et al., 2015) that was previously isolated and identified from *B. acerifolius* (Zeid et al., 2017), *B. rupestris* (Thabet et al., 2018a) and *B. populneus* (Ragheb et al., 2019).

Compound 8 was isolated as a black powder, which appeared on PC as a dark purple spot that converted yellow upon reaction with $AlCl_3$. The ESI-MS spectrum (negative mode) exhibited three peaks at *m/z* 593, corresponding to the molecule ion peak [M-H]$^-$ which was consistent with the molecular formula of $C_{27}H_{29}O_{15}$. Additionally, two daughter ions were observed at *m/z* 447 [M-H-146]$^-$ and 285 [M-H-146-162]$^-$, resulting from the loss of rhamnosyl and glucosyl moieties, respectively. The ^{1}H-NMR (DMSO-d_6) displayed the characteristic signals of flavonol glycoside; two doublet signals resonated at δ_H 6.21 and 6.43 ppm corresponding to the *meta*-coupled aromatic protons of ring A which are 6-H and 8-H, respectively. Two doublets for ortho- coupled protons of ring B at δ_H (ppm) 6.89 (d, J = 7.7 Hz, 2H, 3′-H and 5′-H) and 7.98 (d, J = 8.2 Hz, 2H, 2′-H and 6′-H) characteristic for 1,4-disubstituted benzene ring which revealed that the aglycone part is kaempferol. It also had two anomeric protons at δ_H (ppm) 5.31 (d, J = 7.1 Hz, 1H, 1″-Glu) and 5.09 (d, 1H, 1‴-Rha) in addition to a doublet signal at δ_H 1.05 ppm assigned for the three protons of methyl group of rhamnose sugar which indicated that the glycosyl moiety is rutinoside. The ^{13}C-NMR (DMS*O*-d_6) displayed 25 signals; 13 signals assigned for the kaempferol aglycone and 12 signals for the 3-*O*-rutinoside moiety (3-*O*-(6″-*O*-α-L-rhamnopyranosyl)-β-D-glucopyranoside). Additionally, the glycosylation of C-3 was evidenced by the downfield shift of C-2 and C-4 and the upfield shift of C-3 in comparison with the aglycone spectrum. Compound **8** was identified as nicotiflorin (Cardoso et al., 2005; Wan et al., 2011; Dehaghani et al., 2017), which was previously isolated from *B. rupestris* (El-Sherei et al., 2016; Thabet et al., 2018a) and *B. populneus* (Ragheb et al., 2019).

The HPLC profile of the methanol extract from the leaves of *B. rupestris* was obtained by injecting it at a known concentration into an RP-HPLC-DAD system. The purified compounds were also injected at known concentrations to confirm their purity and to calculate their approximate concentrations in both the crude extract and the fractions from which they were isolated. This data can be obtained by determining the retention times at which the pure compounds were eluted and analyzing the area under the peaks in the chromatograms.

HPLC-DAD analyses of the crude extract and the pure isolated compounds are presented in Table 1. Methyl gallate (1.0 mg/mL) was eluted at 13.50 min., with concentrations in the crude extract and the ethyl acetate fraction measured at 2.80 and 61.85 mg/g, respectively. Caffeic acid (1.0 mg/mL) was detected at 15.60 min., showing concentrations of 7.26 mg/g in the crude extract and 89.61 mg/g in the ethyl acetate fraction. *p*-Coumaric acid (1.0 mg/mL) was identified at 19.10 min., with concentrations of 3.98 mg/g in the crude extract and 48.33 mg/g in the ethyl acetate fraction. Isoquercetin (1.0 mg/mL) was found at 28.02 min., with concentrations of 4.23 mg/g in the crude extract and 26.87 mg/g in the ethyl acetate fraction. Nicotiflorin (1.0 mg/mL) was detected at 35.84 min., with concentrations of 1.06 mg/g in the crude extract and 9.88 mg/g in the *n*-butanol fraction. Quercetin (1.0 mg/mL) was identified at 47.07 min., with concentrations of 0.11 mg/g in the crude extract and 0.67 mg/g in the *n*-butanol fraction. Kaempferol (1.0 mg/mL), isolated from the ethyl acetate-derived fraction, was found at 59.52 min. Rutin (1.0 mg/mL) was found at 27.59 min., with concentrations of 0.48 mg/g in the plant methanol extract and 15.20 mg/g in the *n*-butanol-derived

Table 1. Pure compounds isolated from *B. rupestris* leaves and their retention time and concentration in both methanol extract and derived fraction.

Fraction	Compound	R_t (min)	Conc. (mg/g MeOH extract)	Conc. (mg/g fraction)
EtOAc fraction	Methylgallate	13.50	2.80	61.85
	Caffeic acid	15.60	7.26	89.61
	p-Coumaric acid	19.10	3.98	48.33
	Isoquercetin	28.02	4.23	26.87
	Kaempferol	59.52	—	—
n-BuOH fraction	Rutin	27.59	0.48	15.20
	Nicotiflorin	35.84	1.06	9.88
	Quercetin	47.07	0.11	0.67

fraction. The UV spectrum of each compound was recorded and was in complete agreement with our previous UV analyses and the previously reported data. According to the aforementioned data, the most abundant phytochemicals in the ethyl acetate fraction were caffeic acid, followed by methyl gallate, while rutin was the most predominant in the *n*-butanol fraction. Furthermore, the most prevalent phytochemicals in the crude methanol extract were caffeic acid, followed by isoquercetin. It was observed that the ethyl acetate-derived fraction was richer in phytochemical composition than the *n*-butanol fraction.

The antioxidant activity of the pure isolated compounds was investigated through *in-vitro* antioxidant assay; DPPH$^{\cdot}$ scavenging potential and the results were presented in Table 2. The IC_{50} value of the isolated pure compounds against DPPH$^{\cdot}$ ranged between 18.19 ± 0.161 and 39.11 ± 0.137 µg/mL for methyl galate and rutin, respectively. Methyl gallate possessed the strongest antioxidant activity among the studied compounds with an IC_{50} value of 18.19 ± 0.161 µg/mL against DPPH$^{\cdot}$ followed by the mixture of caffeic acid and *p*-coumaric acid whose IC_{50} value was found to be 18.57 ± 0.123 µg/mL against DPPH$^{\cdot}$. The strong antioxidant activity of the ethyl acetate derived fraction could be attributed to its content of methyl gallate, caffeic acid and *p*-coumaric acid. These compounds could represent promising natural antioxidant alternatives in food, nutraceutical, cosmetic and pharmaceutical industries. Aside from the significant antioxidant potential of the isolated phenolic compounds, many research papers have focused on studying their therapeutic activities. The various biological activities of the isolated compounds are summarized in Table 3, which suggest their valuable application as drugs and prodrugs in the treatment of various ailments. Extensive *in-vitro*, *in-vivo* and clinical studies are still demanded to establish effective safety profile in order to obtain the maximum therapeutic benefits of these compounds.

Table 2. Pure compounds isolated from *B. rupestris* leaves, their antioxidant potential via DPPH$^{\cdot}$ scavenging activity.

Compound	**DPPH antioxidant activity (SC_{50} µg/mL)**
Methyl gallate	18.19±0.161
Caffeic acid	Mix, 18.57±0.123
p-Coumaric acid	
Isoquercetin	31.83±0.302
Rutin	39.11±0.137
Nicotiflorin	26.61±0.225
Ascorbic acid	6.44±0.03

The results are represented as mean of three analyses ± SD.

Table 3. Biological properties of compounds isolated from *B. rupestris* leaves.

Compound	**Biological properties**	**Ref.**
Methyl gallate	Anti-spasmodic, anti-atherogenic, anti-inflammatory, antimicrobial, antidiabetic, neuroprotective, cardiovascular protective, and anticancer	Huang et al. (2021)
Caffeic acid	Anticancer, anti-inflammatory, antimicrobial, antidiabetic, anti-atherosclerotic, and hepatoprotective	Espíndola et al. (2019)
p-Coumaric acid	Anticancer, anti-arthritis, antimicrobial, anti-inflammatory, antiplatelet aggregation, anxiolytic, antipyretic, analgesic, anti-obesity, antidiabetic, hypolipidemic, and anticancer	Pei et al. (2016)
Isoquercetin	Anti-inflammatory, anti-cancer, cardio-protective, antidiabetic, anti-allergic, neuroprotective, and antiviral	Valentová et al. (2014), Orfali et al. (2016), and Magar et al. (2020)
Rutin	Anticancer, antimicrobial, antidiabetic, anti-hypercholesterolemic, neuroprotective, anti-arthritis, analgesic, antihypertensive, antidiabetic, anticoagulant, antiplatelet aggregation, antiulcer, anti-asthmatic, anti-osteoporotic, anti-cataract, cardio-protective, hepato-protective, and nephroprotective	Ganeshpurkar et al. (2017)
Nicotiflorin	Anti-inflammatory, neuroprotective, hepatoprotective, antimicrobial, analgesic, cardio-protective, and nephroprotective	Zhao et al. (2017), Wang et al. (2021), and Yu et al. (2021)

4. Concluding remarks

Few studies were performed to investigate the phytochemical composition and the biological activities of *B. rupestris* leaves. Some of the bioactive phytoconstutients existed in the ethyl acetate and the *n*-butanol fractions derived from the plant crude extract were separated through application of different chromatographic techniques and their chemical structures were elucidated based on different spectroscopic analyses. Eight compounds were isolated in pure form. To the best of our knowledge, this is the first study to report the isolation and the identification of methyl gallate and caffeic acid from *B. rupestris* leaves. Moreover, the antioxidant power of the isolated pure compounds was investigated *in-vitro* against DPPH·. According to the results obtained, *B. rupestris* leaves are a promising alternative source of phenolics with significant antioxidant potential. Further research is required to explore additional therapeutic potential of *B. rupestris* leaves and its bioactive constituents, including *in-vitro* and *in-vivo* studies.

Authors contributions
All authors contributed to data analysis and interpretation, revised the article, provided final approval for the version to be published, and agreed to be accountable for all aspects of the work. Eman Ahmed El-Wakil, Maher Mahmoud El-Hashash, and El-Sayed Saleh Abdel-Hameed conceived and supervised the study. Heba Raafat Mohamed conducted the experimental work and wrote the initial draft of the manuscript.

Availability of data and materials
The data that support the findings of this study are available from the corresponding author, upon reasonable request.

Conflict of interests
The author declare that they have no known competing financial interests or personal relationships that could have appeared to influence the work reported in this paper.

References

Aisyah, L.S., Yun, Y.F., Herlina, T., Julaeha, E., Zainuddin, A., Nurfarida, I., Hidayat, A.T., Supratman, U., Shiono, Y. (2017) Flavonoid compounds from the leaves of *Kalanchoe prolifera* and their cytotoxic activity against P-388 murine leukimia cells. *Nat. Prod. Sci.* 23(2):139–145.
DOI: https://doi.org/10.20307/nps.2017.23.2.139.

Anish, R.J., Rumaisa, F., Aswathy, T.R., Kalpana, V.N.S., Rauf, A.A. (2023) Molecular docking, anti-inflammatory, antimicrobial and antioxidant evaluation of *Pterospermum rubiginosum* B. Heyne. *Trends Phytochem. Res.* 7(2):95–109.
DOI: https://doi.org/10.30495/tpr.2023.1977515.1316.

Atta, E.M., Mohamed, N.H., Abdelgawad, A.A.M. (2017) Antioxidants: An overview on the natural and synthetic types. *Eur. Chem. Bull.* 6(8):365–375.
DOI: https://doi.org/10.17628/ecb.2017.6.365-375.

Cardoso, C.L., Silva, D.H.S., Castro-Gamboa, I., Bolzani V.D.S. (2005) New biflavonoid and other flavonoids from the leaves of *Chimarrhis turbinata* and their antioxidant activities. *J. Braz. Chem. Soc.* 16(6 B):1353–1359.
DOI: https://doi.org/10.1590/S0103-50532005000800008.

Dehaghani, Z.A., Asghari, G., Dinani, M.S. (2017) Isolation and Identification of nicotiflorin and narcissin from the aerial parts of *Peucedanum aucheri* Boiss. *J. Agric. Sci. Technol A.* 7:45–51.
DOI: https://doi.org/10.17265/2161-6256/2017.01.007.

El-Sherei, M.M., Ragheb, A.Y., Kassem, M.E., Marzouk, M.M., Mosharrafa, S.A., Saleh, N.A. (2016) Phytochemistry, biological activities and economical uses of the genus *Sterculia* and the related genera: A reveiw. *Asian. Pac. J. Trop. Dis.* 6(6):492–501.
DOI: https://doi.org/10.1016/S2222-1808(16)61075-7.

Espíndola, K.M.M., Ferreira, R.G., Narvaez, L.E.M., Rosario, A.C.R.S., Silva Da, A.H.M., Silva, A.G.B., Vieira, A.P.O., Monteiro, M.C. (2019) Chemical and pharmacological aspects of caffeic acid and its activity in hepatocarcinoma. *Front. Oncol.* 9:541.
DOI: https://doi.org/10.3389/fonc.2019.00541.

Farag, M.A., Zeid Abou, A.H., Hamed, M.A., Kandeel, Z., El-Rafie, H.M., El-Akad, R.H. (2014) Metabolomic fingerprint classification of *Brachychiton acerifolius* organs via UPLC-qTOF-PDA-MS analysis and chemometrics. *Nat. Prod. Res.* 29(2):116–124.
DOI: https://doi.org/10.1080/14786419.2014.964710.

Ganbaatar, C., Gruner, M., Mishig, D., Duger, R., Schmidt, A.W., Knölker, H-J. (2015) Flavonoid glycosides from the aerial parts of *Polygonatum odoratum* (Mill.) Druce growing in Mongolia. *Open Nat. Prod. J.* 8(1):1–7.
DOI: https://doi.org/10.2174/1874848101508010001.

Ganeshpurkar, A., Saluja, A.K. (2017) The pharmacological potential of rutin. *Saudi Pharm. J.* 25(2):149–164.
DOI: https://doi.org/10.1016/j.jsps.2016.04.025.

Gurivelli, P., Katta, S. (2023) Unlocking the anthelmintic potential of *Grewia bilamellata* Gagnep: *In-vitro* and molecular docking studies on adult Indian earthworms. *Trends Phytochem. Res.* 7(2):127–140.
DOI: https://doi.org/10.30495/tpr.2023.1983640.1332.

Huang, C.Y., Chang, Y.J., Wei, P.L., Hung, C.S., Wang, W. (2021) Methyl gallate, gallic acid-derived compound, inhibit cell proliferation through increasing ROS production and apoptosis in hepatocellular carcinoma cells. *PLoS ONE* 16(3):e0248521.
DOI: https://doi.org/10.1371/journal.pone.0248521.

Iwashina, T., Tamura, M.N., Murai, Y., Kitajima, J. (2013) New flavonol glycosides from the leaves of *Triantha japonica* and *Tofieldia nuda*. *Nat. Prod. Commun.* 8(9):1251–1254.
DOI: https://doi.org/10.1177/1934578x1300800917.

Jeong, C.H., Jeong, H.R., Choi, G.N., Kim, D.O., Lee, U., Heo, H.J. (2011) Neuroprotective and anti-oxidant effects of caffeic acid isolated from *Erigeron annuus* leaf. *Chin. Med.* 6(25):1–9.
DOI: https://doi.org/10.1186/1749-8546-6-25.

Liu, H., Mou, Y., Zhao, J., Wang, J., Zhou, L., Wang, M., Wang, D., Han, J., Yu, Z., Yang, F. (2010) Flavonoids from *Halostachys caspica* and their antimicrobial and antioxidant activities. *Molecules* 15(11):7933–7945.
DOI: https://doi.org/10.3390/molecules15117933.

Lubis, M.Y., Siburian, R., Marpaung, L., Simanjuntak, P., Nasution, M.P. (2018) Methyl gallate from Jiringa (*Archidendron jiringa*) and antioxidant activity. *Asian J. Pharm. Clin. Res.* 11(1):346–350.
DOI: https://doi.org/10.22159/ajpcr.2018.v11i1.21637.

Magar, R.T., Sohng, J.K. (2020) A review on structure, modifications and structure-activity relation of quercetin and its derivatives. *J. Microbiol. Biotechnol.* 30(1):11–20.
DOI: https://doi.org/10.4014/jmb.1907.07003.

Manivannan, R., Shopna, R. (2015) Isolation of quercetin and isorhamnetin derivatives and evaluation of anti-microbial and anti-inflammatory activities of *Persicaria glabra*. *Nat. Prod. Sci.* 21(3):170–175.

Mohamed, H.R., Abdel-Hameed, E.S., El-Wakil, E.A., El-Hashash, M.M., Shemis, M. (2021) Phytochemical screening, *in-vitro* antioxidant and cytotoxic potentials of *Brachychiton rupestris* leaves. *Res. J. Pharm. Technol.* 14(6):3119–3127.
DOI: https://doi.org/10.52711/0974-360X.2021.00544.

Mohamed, H.R., El-Wakil, E.A., El-Hashash, M.M., Abdel-Hameed, E.S.S. (2023) Chemical constituents of *Ailanthus altissima* (Mill.) swingle leaves growing in Egypt and their antioxidant activity. *Acta Pharm. Sci.* 61(3):213–233.
DOI: https://doi.org/10.23893/1307-2080.APS6115.

Mohammadhosseini, M., Frezza, C., Venditti, A., Sarker, S.D. (2021) A systematic review on phytochemistry, ethnobotany and biological activities of the genus *Bunium* L. *Chem. Biodivers.* 18(11):e2100317.
DOI: https://doi.org/10.1002/cbdv.202100317.

Mohammadhosseini, M., Jeszka-Skowron, M. (2023) A systematic review on the ethnobotany, essential oils, bioactive compounds, and biological activities of *Tanacetum* species. *Trends Phytochem. Res.* 7(1):1–29.
DOI: https://doi.org/10.30495/tpr.2023.700612.

Olennikov, D.N., Chirikova, N.K. (2018) Rhamnetin glycosides from the genus *Spiraea*. *Chem. Nat. Compd.* 54(1):41–45.
DOI: https://doi.org/10.1007/s10600-018-2255-9.

Oliveira De, D.M., Siqueira, E.P., Nunes, Y.R.F., Cota, B.B. (2013) Flavonoids from leaves of *Mauritia flexuosa*. *Rev. Bras. Farmacogn.* 23(4):614–620.
DOI: https://doi.org/10.1590/S0102-695X2013005000061.

Orfali, G.C., Duarte, A.C., Bonadio, V., Martinez, N.P., Araújo de, M.E.M.B., Priviero, F.B.M., Carvalho, P.O., Priolli, D.G. (2016) Review of anticancer mechanisms of isoquercitin. *World J. Clin. Oncol.* 7(2):189–199.
DOI: https://doi.org/10.5306/wjco.v7.i2.189.

Pei, K., Ou, J., Huang, J., Ou, S. (2016) *p*-Coumaric acid and its conjugates: Dietary sources, pharmacokinetic properties and biological activities. *J. Sci. Food Agric.* 96(9):2952–2962.
DOI: https://doi.org/10.1002/jsfa.7578.

Phaniendra, A., Jestadi, D.B., Periyasamy, L. (2015) Free radicals: Properties, sources, targets, and their implication in various diseases. *Indian J. Clin. Biochem.* 30(1):11–26.
DOI: https://doi.org/10.1007/s12291-014-0446-0.

Ragheb, A.Y., Kassem, M.E.S., El-Sherei, M.M., Marzouk, M.M., Mosharrafa, S.A., Saleh, N.A.M. (2019) Morphological, phytochemical and anti-hyperglycemic evaluation of *Brachychiton populneus*. *Rev. Bras. Farmacogn.* 29:559–569.
DOI: https://doi.org/10.1016/j.bjp.2019.05.001.

Rjeibi, I., Saad Ben, A., Ncib, S., Souid, S., Allagui, M.S., Hfaiedh, N. (2020) *Brachychiton populneus* as a novel source of bioactive ingredients with therapeutic effects: antioxidant, enzyme inhibitory, anti-inflammatory properties and LC-ESI-MS profile. *Inflammopharmacology* 28(2):563–574.
DOI: https://doi.org/10.1007/s10787-019-00672-8.

Thabet, A.A., Youssef, F.S., El-Shazly, M., El-Beshbishy, H.A., Singab, A.B. (2018a) Validation of the antihyperglycaemic and hepatoprotective activity of the flavonoid rich fraction of *Brachychiton rupestris* using *in vivo* experimental models and molecular modelling. *Food Chem. Toxicol.* 114:302–310.
DOI: https://doi.org/10.1016/j.fct.2018.02.054.

Thabet, A.A., Youssef, F.S., El-Shazly, M., Singab, A.B. (2017) Antiinfective properties of *Brachychiton rupestris* and *Brachychiton luridum* Leaves and their qualitative phytochemical screening. *Med. Aromat. Plants.* 6(4):1000299.
DOI: https://doi.org/10.4172/2167-0412.1000299.

Thabet, A.A., Youssef, F.S., Korinek, M., Chang, F., Wu, Y., Chen, B., El-Shazly, M., Singab, A., Hwang, T. (2018b) Study of the antiallergic and anti-inflammatory activity of *Brachychiton rupestris* and *Brachychiton discolor* leaves (Malvaceae) using *in vitro* models. *BMC Complement. Altern. Med.* 18(1):299.
DOI: https://doi.org/10.1186/s12906-018-2359-6.

Thagriki, D.S., Ray, U. (2022) An overview of traditional medicinal plants as dengue virus inhibitors. *Trends Phytochem. Res.* 6(2):116–136.
DOI: https://doi.org/10.30495/tpr.2022.1956618.1254.

Valentová, K., Vrba, J., Bancířová, M., Ulrichová, J., Křen, V. (2014) Isoquercitrin: Pharmacology, toxicology, and metabolism. *Food Chem. Toxicol.* 68:267–282.
DOI: https://doi.org/10.1016/j.fct.2014.03.018.

Wan, C., Yu, Y., Zhou, S., Tian, S., Cao, S. (2011) Isolation and identification of phenolic compounds from *Gynura divaricata* leaves. *Pharmacogn. Mag.* 7(26):101–108.
DOI: https://doi.org/10.4103/0973-1296.80666.

Wang, L., Li, C., Guan, C., Zhang, Y., Yang, C., Zhao, L., Luan, H., Zhou, B., Che, L., Wang, Y., Zhang, W., Zhang, H., Man, X., Jiang, W., Xu, Y. (2021) Nicotiflorin attenuates cell apoptosis in renal ischemia-reperfusion injury through activating transcription factor 3. *Nephrology* 26(4):358–368.
DOI: https://doi.org/10.1111/nep.13841.

Wang, Y., Wray, V., Tsevegsuren, N., Lin, W., Proksch, P. (2012) Phenolic compounds from the Mongolian medicinal plant *Scorzonera radiata*. *Z. Naturforsch. C. J. Biosci.* 67 C(3-4):135–143.
DOI: https://doi.org/10.1515/znc-2012-3-405.

Yasir, M., Sultana, B., Amicucci, M. (2016) Biological activities of phenolic compounds extracted from Amaranthaceae plants and their LC/ESI-MS/MS profiling. *J. Funct. Foods* 26:645–656.
DOI: https://doi.org/10.1016/j.jff.2016.08.029.

Yu, S., Guo, Q., Jia, T., Zhang, X., Guo, D., Jia, Y., Li, J., Sun, J. (2021) Mechanism of action of nicotiflorin from *Tricyrtis maculata* in the treatment of acute myocardial Infarction: From network pharmacology to experimental pharmacology. *Drug Des. Devel. Ther.* 15:2179–2191.
DOI: https://doi.org/10.2147/DDDT.S302617.

Zeid Abou, A.H., Farag, M.A., Hamed, M.A.A., Kandil, Z.A.A., El-Akad, R.H., El-Rafie, H.M. (2017) Flavonoid chemical composition and antidiabetic potential of *Brachychiton acerifolius* leaves extract. *Asian Pac. J. Trop. Biomed.* 7(5):389–396.
DOI: https://doi.org/10.1016/j.apjtb.2017.01.009.

Zhao, J., Zhang, S., You, S., Liu, T., Xu, F., Ji, T., Zhengyi, G. (2017) Hepatoprotective effects of nicotiflorin from *Nymphaea candida* against concanavalin A-induced and D-galactosamine-induced liver injury in mice. *Int. J. Mol. Sci.* 18(3):587.
DOI: https://doi.org/10.3390/ijms18030587.